

Lifetime estimations and a non-monotonic initial energy density in heavy ion collisions at RHIC and LHC

G. Kasza^{a,b 1}, *T. Csörgő*^{a,b,c 2}

^a MTA Wigner FK, H-1525 Budapest 114, P.O.Box 49, Hungary

^b EKE KRC, H-3200 Gyöngyös, Mátrai út 36, Hungary

^c CERN, CH-1211 Geneva 23, Switzerland

We highlight some connections between the final state hadronic observables and the initial conditions using a recently found new exact family of solutions of relativistic hydrodynamics. These relations provide explicit examples of the scaling behaviour in relativistic hydrodynamics and may provide an advanced estimate of the lifetime and the initial energy density in $\sqrt{s_{NN}} = 62.4, 130, \text{ and } 200 \text{ GeV}$ Au+Au collisions at RHIC and $\sqrt{s_{NN}} = 5.0 \text{ TeV}$ Pb+Pb and 5.44 TeV Xe+Xe as well as $\sqrt{s} = 7, 8 \text{ and } 13 \text{ TeV}$ p+p collisions at LHC energies. A surprising result is that these advanced estimates yield a non-monotonic increase of the initial energy density with increasing collision energy at the RHIC energy range.

Introduction

Recently, we have published a series of manuscripts that presents a new family of exact solutions of relativistic hydrodynamics [1], and its applications to the evaluation of the pseudorapidity distributions [2], the longitudinal HBT radii [3], the estimation of the initial energy densities [4] as well as the application of these results to the analysis of experimental data at RHIC and LHC energies [5]. In this conference contributions we highlight some of the most beautiful results, that are given in full detailed in refs. [1–5].

New, exact solutions of relativistic, perfect fluid hydrodynamics

The equations of relativistic perfect fluid hydrodynamics are given in terms of the entropy density, denoted by σ , the four velocity u^μ , normalized as $u^\mu u_\mu = 1$, and the energy-momentum four tensor $T^{\mu\nu}$, as follows. These fields depend on $x \equiv x^\mu = (t, r_x, r_y, r_z)$.

$$\partial_\mu (\sigma u^\mu) = 0, \quad (1)$$

$$\partial_\nu T^{\mu\nu} = 0. \quad (2)$$

¹E-mail: kasza.gabor@wigner.mta.hu

²E-mail: tcsorgo@cern.ch

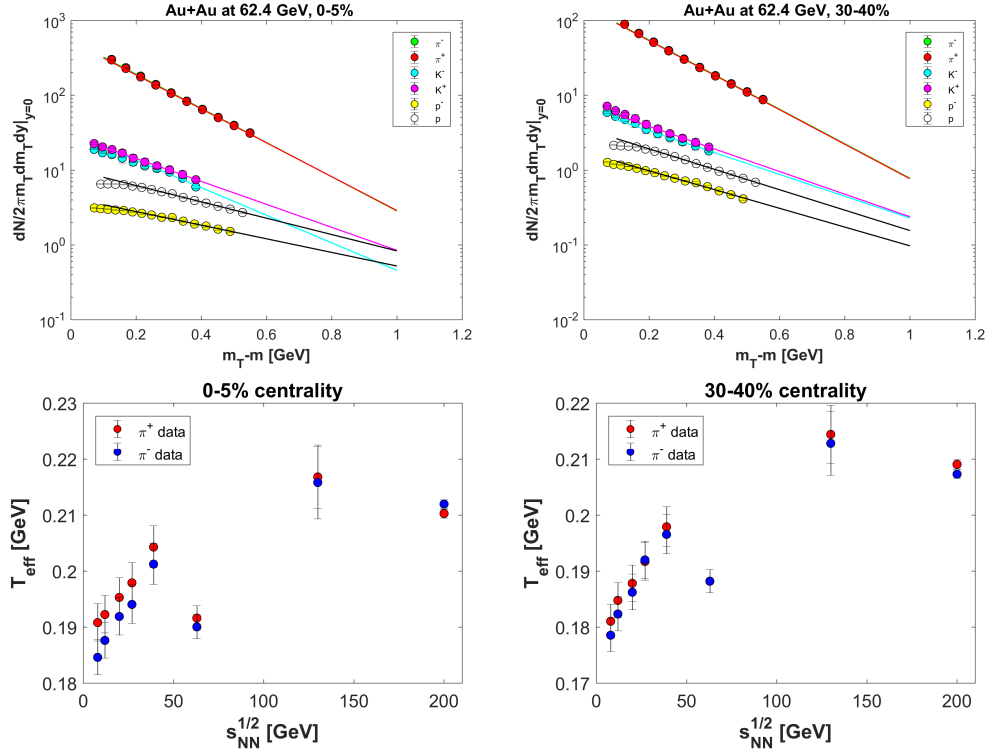


Fig. 1. The top left panel indicates the result of fits with $A \exp[-(m_T - m)/T_{\text{eff}}]$ to the invariant momentum distribution of π^\pm , K^\pm , p and \bar{p} to $\sqrt{s_{NN}} = 62.4$ GeV Au+Au collisions in the 0–5 % centrality class. The top right panel shows the same in the 30–40 % centrality class. Bottom left panel shows the excitation function of the effective temperature of positively and negatively charged pions in the 0–5 % centrality class. Bottom right panel shows the same in the 30–40 % centrality class. The bottom panels are indicating a non-monotonic behaviour of the pion slope parameters with increasing energy, in both centrality classes.

For perfect fluids, the energy-momentum four tensor is

$$T^{\mu\nu} = (\varepsilon + p) u^\mu u^\nu - p g^{\mu\nu}, \quad (3)$$

where $\varepsilon \equiv \varepsilon(x)$ is the energy density and $p \equiv p(x)$ is the pressure, and $g^{\mu\nu} = \text{diag}(1, -1, -1, -1)$ stands for the Minkowskian metric. The above set of equations is closed by the following equation of state:

$$p = \bar{c}_s^2 \varepsilon = \varepsilon/\kappa, \quad (4)$$

where $\bar{c}_s \equiv 1/\sqrt{\kappa}$ is a temperature independent, average value of the speed of sound, that was measured by the PHENIX collaboration in ref. [7]: $\bar{c}_s = 0.35 \pm 0.05$, corresponding to $\kappa = 10_{-3}^{+1}$. An exact and analytic, finite and accelerating, 1+1 dimensional solution of relativistic perfect fluid hydrodynamics was recently found by Csörgő, Kasza, Csanád and Jiang (CKCJ) [1] as a family of parametric curves, obtained by using the Rindler-

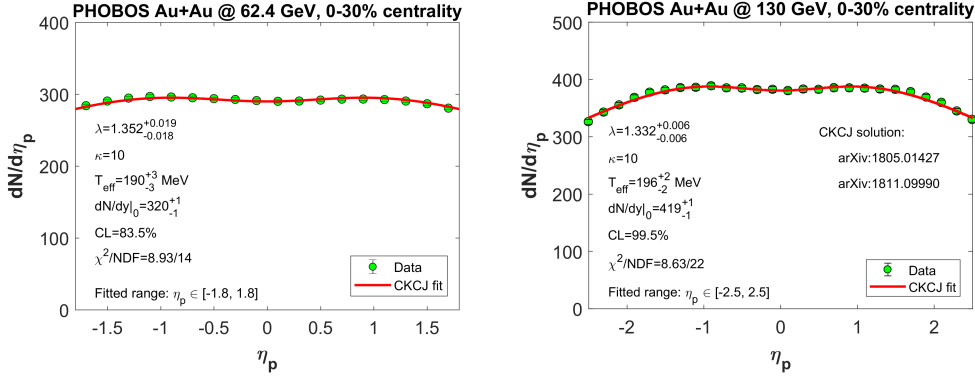


Fig. 2. Description of PHOBOS results [6] on the pseudorapidity distributions of $\sqrt{s_{NN}} = 62.4$ and 130 GeV, 0-30 % Au+Au collisions with the CKCJ solutions of relativistic hydrodynamics, using eqs. (5-7). Details of the fitting method are described in ref. [5].

coordinates: $(\tau, \eta_x) = \left(\sqrt{t^2 - r_z^2}, \frac{1}{2} \ln \left[\frac{t+r_z}{t-r_z} \right] \right)$, where τ stands for the longitudinal proper time and η_x is the space-time rapidity. The four-velocity is chosen as $u^\mu = (\cosh(\Omega), \sinh(\Omega))$ and it was assumed that the fluid rapidity $\Omega \equiv \Omega(\eta_x)$ is independent of the proper time. The new class of CKCJ solutions was presented in ref. [1] and the corresponding pseudorapidity distributions were obtained as parametric curves in ref. [2].

We present this formulae, as well as an advanced estimation of the initial energy densities [4], and the results on the longitudinal HBT radii of ref. [3], as derived from the CKCJ exact solution of relativistic hydrodynamics. This solution is an explicit function of the longitudinal proper-time τ , while its dependence on the space-time rapidity η_x is given in terms of parametric curves, parameterized in terms of $H = \Omega - \eta_x$. These solutions are constrained to a cone inside the forward lightcone, limited by constant pseudorapidity lines, see ref. [1] for details.

Pseudorapidity density and hydrodynamic scaling behaviour

Recently, a robust functional form has been derived [5] from the CKCJ solution [1]:

$$\frac{dN}{d\eta_p} \approx \frac{\langle N \rangle}{(2\pi\Delta^2 y)^{1/2}} \frac{\cosh(\eta_p)}{[(m/\bar{p}_T)^2 + \cosh^2(\eta_p)]^{1/2}} \exp\left(-\frac{y^2}{2\Delta^2 y}\right) \Big|_{y=y(\eta_p)}, \quad (5)$$

$$\frac{1}{\Delta^2 y} = (\lambda - 1)^2 \left[1 + \left(1 - \frac{1}{\kappa}\right) \left(\frac{1}{2} + \frac{m}{T_{\text{eff}}}\right) \right], \quad (6)$$

$$y(\eta_p) \approx \tanh^{-1} \left(\sinh(\eta_p) / \sqrt{(m/\bar{p}_T)^2 + \cosh^2(\eta_p)} \right). \quad (7)$$

This formula can be used to fit the pseudorapidity density distributions at RHIC and LHC energies from proton-proton to (symmetric) heavy ion collisions near mid-rapidity, outside the spectator fragmentation regions, where possible shock-wave effects might

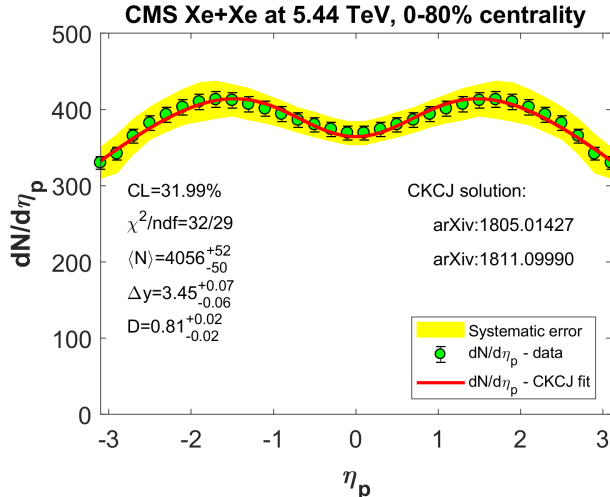


Fig. 3. Fits of the pseudorapidity density with the CKCJ hydro solution [1], to CMS Xe+Xe data at $\sqrt{s_{NN}} = 5.44$ TeV [12] in the 0-80 % centrality class, using eqs. (5,6,7) [5]. The fit parameters are the mean multiplicity $\langle N \rangle$, the Gaussian width of Δy and the dimensionless dip parameter $D = m/\bar{p}_T$. Yellow band stands for the systematic errors of ref. [12].

have to be taken into account too. Here parameter λ is a constant of integration, that controls the width of the pseudorapidity distribution. It can be determined from fits to the pseudorapidity distribution data. Given that Δy is a physical fit parameter, that corresponds to a combination of the equation of state parameter κ , the mass m of the particles (predominantly pions), and T_{eff} is the slope parameter of the single-particle spectra, eq. (6) is a beautiful example of the hydrodynamical scaling behaviour: different hydrodynamical sources may lead to the same pseudo-rapidity distributions, if the relevant combination Δy of the hydrodynamical parameters λ , κ , m and T_{eff} is the same. The boost-invariant Hwa-Bjorken solution corresponds to the $\lambda \rightarrow 1$ limit. The depression of the pseudorapidity distribution at mid-rapidity is controlled by the average transverse momentum at mid-rapidity, denoted by \bar{p}_T , which together with T_{eff} can also be determined from fits to the transverse mass spectra as indicated on Fig. 1. If $\lambda - 1 \ll 1$, $\bar{p}_T = \sqrt{(m + T_{\text{eff}})^2 - m^2}$, see ref. [5] for more details. The above form of the pseudorapidity distribution is normalized to $\langle N \rangle$, the mean multiplicity. In this case the normalization should also be changed from the infinite mean multiplicity and the diverging Δy to their ratio, the finite mid-rapidity density, given by $\langle N \rangle / (2\pi\Delta^2 y)^{1/2}$.

The CKCJ solution was shown to describe the pseudorapidity density distribution of $p + p$ collisions at $\sqrt{s} = 7$ and 8 TeV in ref. [1]. The description of the pseudorapidity distribution of 40 - 50 % Pb+Pb collisions at $\sqrt{s_{NN}} = 5$ TeV was given in ref. [2], while fits to $Au + Au$ collision data at $\sqrt{s_{NN}} = 200$ GeV were shown in ref. [3]. Several other plots were shown in conference presentations that indicate that the CKCJ solution of relativistic hydrodynamics describes well the pseudorapidity distributions from $p + p$ through $Xe + Xe$ and $Au + Au$ to $Pb + Pb$ collisions, from the colliding energies of $\sqrt{s_{NN}} = 20$ GeV to the presently largest LHC energy of $\sqrt{s} = 13$ TeV. Most recently, we

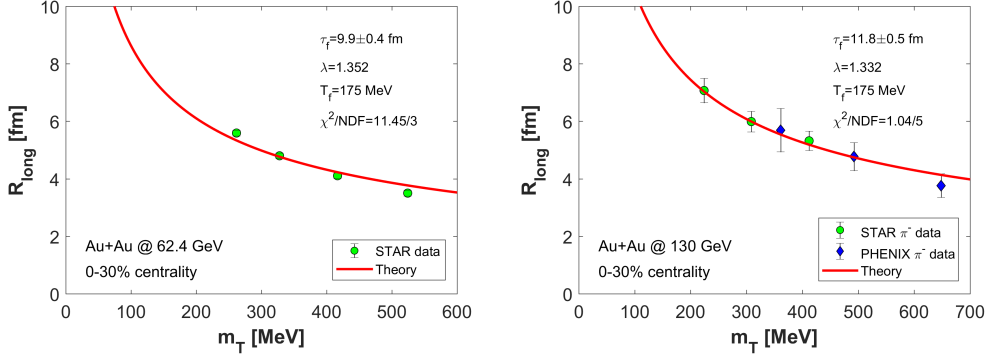


Fig. 4. Fits of the longitudinal HBT-radii with the CKCJ hydro solution [1], to STAR Au+Au data at $\sqrt{s_{NN}} = 62.4$ GeV [8] (left) and to PHENIX and STAR Au+Au data at $\sqrt{s_{NN}} = 130$ GeV [9] (right) in the 0-30 % centrality class, for a fixed centrality class and colliding system.

have described the CMS measurement of the pseudorapidity density in $Xe+Xe$ collisions at $\sqrt{s_{NN}} = 5.44$ TeV [12] in the 0-80 % centrality class, as indicated on Fig. 3.

Life-time and initial energy density estimation at RHIC energies

In this section we present a new method, which is developed to determine the initial energy density of the expanding fireballs, as a function of only one parameter, the initial proper time. These method can be summarized as follows: *(i)* Evaluate the effective temperature (T_{eff}) from fits to the invariant momentum distribution of identified hadrons, as a function of $m_T - m$. *(ii)* Determine the acceleration parameter λ from a fit with eq. (5), by using eqs. (6,7) from fits to measured pseudorapidity density data. See refs. [1,2,5] for details. *(iii)* Fit the m_T dependence of the longitudinal HBT-radii R_{long} , to evaluate the life-time parameter of the medium. This HBT radius parameter was derived from the CKCJ solution in ref. [4] as follows:

$$R_{\text{long}} = \tau_f \Delta\eta_x \approx \frac{\tau_f}{\sqrt{\lambda(2\lambda - 1)}} \sqrt{\frac{T_f}{m_T}}, \quad (8)$$

where τ_f is the life-time parameter, and T_f stands for the kinetic freeze-out temperature. *(iv)* Finally, one can use the fitted parameters to evaluate the initial energy density by our new formula that was calculated exactly from the CKCJ solution. It corrects the Bjorken estimation by taking into account the non boost-invariant expansion and the finite width of the pseudo-rapidity distribution, as represented by $\lambda \neq 1$, as well as the work, done by the pressure during the fireball evolution [3]:

$$\varepsilon_0(\kappa, \lambda) = \varepsilon_0^{\text{Bj}} (2\lambda - 1) \left(\frac{\tau_f}{\tau_0} \right)^{\lambda(1 + \frac{1}{\kappa}) - 1}, \quad (9)$$

where $\varepsilon_0^{\text{Bj}}$ is Bjorken's estimate and it can be expressed as [10]:

$$\varepsilon_0^{\text{Bj}} = \frac{\langle E_T \rangle}{S_\perp \tau_0} \left. \frac{dN}{d\eta_p} \right|_{\eta_p=0}. \quad (10)$$

In this Bjorken estimate, $\langle E_T \rangle$ is the average thermalized, transverse energy and S_\perp stands for the overlap area of the colliding nuclei.

We have gone through on these steps, so we estimated the initial energy density of RHIC Au+Au collisions at 3 different colliding energies, namely: $\sqrt{s_{NN}} = 62.4, 130$ and 200 GeV. Here, we can only highlight one of the surprising results, which indicate an unexpected feature of the strongly interacting quark-gluon plasma (sQGP) created in Au+Au collisions at RHIC energies. Our advanced initial energy density estimate of $\sqrt{s_{NN}} = 130$ and 200 GeV collisions is detailed in ref. [5].

Fig. 5 indicates the initial energy densities as a function of the colliding energies in the 0-30 % centrality class. This figure immediately highlights the surprising feature we have just mentioned. Although Bjorken's estimate suggests a monotonic increase of the initial energy density with increasing energy, our advanced initial energy density estimate indicates a non-monotonic behavior.

This result is to be considered as preliminary and treated carefully, due to the limitations of the CKCJ solution: this solution does not include transverse dynamics, and the temperature dependence of the speed of sound is replaced by an average value. Both shear and bulk viscosity effects are neglected. However, we have cross-checked in ref [5], that our analytical results on the initial energy density yields similar time evolution for the energy density in the center of the fireball to that of an 1+3 dimensional numerical solution of the equations of relativistic hydrodynamics using the lattice QCD equation of state [11]. This comparison provided a surprisingly good agreement, suggesting that the non-monotonic behavior of the initial energy density with increasing energy of the RHIC beam energy scan may be a robust feature of the data. Of course, it is conceivable that the match is a coincidence, since ref. [11] did not made explicit the centrality class of the calculation. In addition, of course, the question may arise about the initial energy density of LHC energies predicted by the CKCJ solution. We have also estimated with our new method the lower limit of the initial energy density of $Pb+Pb$ collisions at $\sqrt{s_{NN}} = 2.76$ TeV, in the 10-20 % centrality class. The result satisfied our expectation, namely the lower limit of the initial energy density at such a high colliding energy is higher than our initial energy density estimate at $\sqrt{s_{NN}} = 200$ GeV, the top RHIC energy for $Au+Au$ collisions.

In summary, we highlighted in this work two of our remarkable theoretical results from ref. [5] :

(i) A simple and beautiful formula was found to describe the pseudorapidity density distribution from the CKCJ solution of relativistic hydrodynamics. This formula is given by eqs. (5-7), and it describes not only $p + p$ and heavy ion data at RHIC and LHC energies, but it also describes excellently the recent CMS data on Xe + Xe collisions exceedingly well.

(ii) We outlined our new method to extract the initial energy density of high energy proton-proton and heavy ion collisions, that corrects Bjorken's oversimplified initial energy density estimate for realistic pseudorapidity density distributions and for taking into

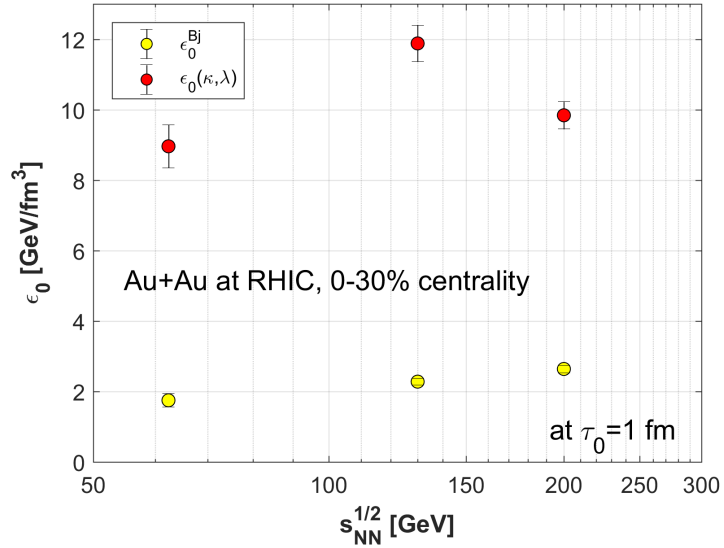


Fig. 5. Initial energy density estimations as a function of the colliding energy. The calculations were performed at 62.4 GeV, 130 GeV and 200 GeV. The red dots stand for the results of our advanced initial energy estimate, based on eq. (9), while the yellow dots correspond to Bjorken's estimate. Our advanced estimates indicate a surprising and non-monotonic behavior of the initial energy density as a function of the collision energy.

account the work done by the non-vanishing pressure during the expansion.

The excitation function of the initial energy density is summarized in Fig. (5), indicating a non-monotonic behaviour. These advanced estimates of the initial energy density may thus become a new tool to search for the critical point of the QCD phase diagram: in the vicinity of the QCD critical point, several quantities may behave in a non-monotonic manner, including life-time related observables, such as the estimated initial energy density. Indeed, a non-monotonic behaviour of the HBT-radii has been observed in the RHIC beam energy scan, pointing to a QCD critical point near $\mu_B \approx 95$ MeV, corresponding to $\sqrt{s_{NN}} \approx 47.5$ GeV [13]. Our data analysis related to the estimations of the initial energy density of Au+Au collisions at RHIC supports independently the possibility of this kind of a scenario. This scenario is also supported by the rather robust nature of Fig. 1, that indicates a non-monotonic dependence of the slope parameters of the single-particle transverse mass spectra on $\sqrt{s_{NN}}$ in a similar energy range.

Further, more detailed studies are necessary to investigate possible shock-wave effects at lower colliding energies, together with the effects arising from a possible proper-time dependence of the acceleration parameter λ and from using a more realistic, 1+3 dimensional expansion, the temperature dependence of the speed of sound and using a lattice QCD equation of state.

Acknowledgments

This research has been partially supported by the NKIFH grants No. FK-123842 and FK-123959, the EFOP 3.6.1-16-2016-00001 grant (Hungary), and THOR, the EU COST Action CA15213.

REFERENCES

1. T. Csörgő, G. Kasza, M. Csanád and Z. Jiang, *Universe* **4** (2018) 69
2. T. Csörgő, G. Kasza, M. Csanád and Z. F. Jiang, *Acta Phys. Pol. B* **50** (2019) p. 27
3. G. Kasza and T. Csörgő, *Acta Phys. Pol. B Proc. Suppl.* v. 12 (2019) p. 175
4. T. Csörgő and G. Kasza, *Acta Phys. Pol. B Proc. Suppl.* v. 12 (2019) p. 217
5. G. Kasza and T. Csörgő, *Int. J. Mod. Phys. A* **34**, no. 26, 1950147 (2019)
6. B. Alver *et al.* [PHOBOS Collaboration], *Phys. Rev. C* **83**, 024913 (2011)
7. A. Adare *et al.* [PHENIX Collaboration], *Phys. Rev. Lett.* **98**, 162301 (2007)
8. L. Adamczyk *et al.* [STAR Collaboration], *Phys. Rev. C* **92**, no. 1, 014904 (2015)
9. K. Adcox *et al.* [PHENIX Collaboration], *Phys. Rev. Lett.* **88** (2002) 192302
10. J. D. Bjorken, *Phys. Rev. D* **27**, 140 (1983).
11. P. Bozek and I. Wyskiel, *Phys. Rev. C* **79** (2009) 044916
12. A. M. Sirunyan *et al.* [CMS Collaboration], arXiv:1902.03603 [hep-ex].
13. R. A. Lacey, *Phys. Rev. Lett.* **114**, no. 14, 142301 (2015)